Anal. Bioanal. Electrochem., Vol. 10, No. 2, 2018, 249-268

Analytical & Bioanalytical Electrochemistry

2018 by CEE
www.abechem.com

Full Paper

Coriandrum Sativum.L Seeds Extract as a Novel Green Corrosion Inhibitor for Mild Steel in 1.0 M Hydrochloric and 0.5 M Sulfuric Solutions

Lamya Kadiri,[1] Mouhsine Galai,[2,*] Moussa Ouakki,[3] Youness Essaadaoui,[1] Abdelkarim Ouass,[1,3] Mohammed Cherkaoui,[3] El-Housseine Rifi[1] and Ahmed Lebkiri[1]

[1]*Laboratory of Organic Synthesis and Extraction Processes, University Ibn Tofail, Faculty of Sciences, Department of Chemistry, PO Box 133 – 14000- 16 Kenitra, Morocco*
[2]*Laboratory of Materials Engineering and Environment: Modelling and Application, University Ibn Tofail, Faculty of Sciences, Department of Chemistry, PO Box 133 – 14000- 16 Kenitra, Morocco*
[3]*Laboratory of Materials, Electrochemistry and Environment, University Ibn Tofail, Faculty of Sciences, Department of Chemistry, PO Box 133 – 14000- 16 Kenitra, Morocco*

*Corresponding Author, Tel.: (+212)677235695
E-Mail: galaimouhsine@gmail.com

Received: 17 October 2017 / Received in revised form: 1 January 2018 / Accepted: 20 January 2018 / Published online: 28 February 2018

Abstract- The comparative study of the inhibition and adsorption properties of extract of *Coriandrum Sativum* seeds (CSE) as a new eco-friendly corrosion inhibition in 1.0 M hydrochloric and 0.5 M sulfuric solutions was investigated using several methods such as polarization curves, Bode plots, electrochemical impedance spectroscopy (EIS) and scanning electron microscopy (SEM). All results demonstrated that CSE suppressed the corrosion reaction in both acids medium (93.7% in 1.0 M HCl, 96.7% in 0.5 M H_2SO_4). Adsorption characteristics of the extract were approximated by various adsorption isotherm models (Langmuir, Freundlich and Temkin) and were in a good agreement with the Fourier Transformed Infrared spectroscopy (FTIR) results, they have shown that CSE contains Functional groups responsible of corrosion inhibition and other methods results.The inhibition mechanisms, estimated from the temperature dependence of inhibition efficiency as well from kinetic and activation parameters show that the extract functioned via mixed inhibition mechanism. It is suggested that molecular as well as protonated organic species in the extract contribute to the observed inhibiting action.

Keywords- *Coriandrum Sativum.L* seeds, Corrosion inhibitor, Mild steel, 1.0 M Hydrochloric acid, 0.5 M Sulfuric acid

1. INTRODUCTION

The unique mechanical properties combined with economic viability of mild steel has made it one of the most important constructional materials in industrial applications including petroleum production and refining, marine applications, chemical processing, construction, metal processing and other industries. However, it has the inconvenient of poor susceptibility towards corrosion in aggressive environments and needs to be protected [1-3].

Acid solutions are also widely used in the industry, the main areas of applications being stripping or cleaning and elimination of localized deposits (rust, bacterial deposits, etc...). The aggressiveness of these acid solutions leads to the use of essential corrosion inhibitors in order to limit the attack of the metallic materials [4].

Historically, synthetic inhibitors had great use in the industries due to their excellent anti-corrosive proprieties. However, many of them cause damages to environment.

The study of organic corrosion inhibition is an alternative field of research due to its usefulness in several industries. Organic heterocyclic compounds contain heteroatoms such as oxygen, nitrogen, sulphur and phosphorous. In addition, they also contain double bonds, triple bonds and aromatic rings. All these enhance the adsorption process and result in the formation of effective coating on the surface of the metal. This coating forms a barrier between metal and the corrosive environment and protects the metal from undergoing corrosion. Various classes of organic inhibitors are successfully used as corrosion inhibitors till date [5].

The exploration of natural extracts of plant origin as corrosion inhibitors is an essential field of research. In addition to being environmentally friendly and ecologically acceptable, plant products are cheap and renewable sources corrosion inhibitors. Therefore, the uses of plant extracts as corrosion inhibitors are due to their economic and environmental benefits. Many plant extracts have been used as effective corrosion inhibitors of mild steel in both acidic and alkaline medium [6], such as *UAES crophularia Arguta* [7], *Aloe vera* [8], *Phyllanthusamarus* [9], *Chamaeropshumilis* [10], *Gossipiumhirsutum L.* [11], *and Cinnamon* [12].

Indeed, these natural extracts usually contain many families of natural organic compounds (flavonoids, alkaloids, tannins...) "ecological", easily available, biodegradable and renewable [4].

Coriandrum Sativum L. known as Coriander is an annual herb in the family of Apiaceae. Seeds are most traditionally used in cooking. Also, it is a rich source of antioxidant and has lots of medicinal applications. It contains several biodegradable ecologically acceptable organic compounds [1].

The aim of the present work is the investigation of Moroccan *Coriandrum Sativum L.* seeds extracts (CSE) as a novel green inhibitor for corrosion control of mild steel in 1.0M hydrochloric and 0.5M sulfuric acid solutions. In fact CSE contains oxygen atoms and functional groups attached to aromatic ring, which are commonly found in corrosion inhibitors according to the characterization results by Fourier Transformed Infrared spectroscopy (FTIR). It is in this context that an electrochemical study has been realised using several spectroscopic and electrochemical techniques such as Tafelpolarization curves, electrochemical impedance spectroscopy (EIS), Bode plots and scanning electron microscopy (SEM). The modelling of the isotherms and the thermodynamic study of adsorption was explored in order to evaluate and define the adsorption process type.

2. MATERIAL AND METHODS

2.1. Specimen preparation

Corrosion experiments were performed on mild steel specimen with weight percentage of each chemical compound as follows in Table 1.

Table 1. Weight and chemical composition of studied mild steel

Element	**Fe**	**Mn**	**Si**	**Cu**	**Cr**	**C**	**Ni**	**W**	**Al**	**Mo**	**V**	**Co**
Weight (%)	98.7	0.47	0.24	0.14	0.12	0.11	0.10	0.06	0.03	0.02	<0.003	0.0012

Samples were mechanically cut to coupons of dimension 1×1 cm, then polished using different grades (from 180 to 2000 grade) emery papers before each test, cleaned by distilled water and acetone, degreased in ethanol and dried with hot air.

Fig. 1. *Coriandrum Sativum* seeds

2.2. Material

Coriandrum Sativum seeds were washed to remove impurities such as sand and dust; they were dried at 50 °C to prevent a possible alteration of the physical and chemical properties of the material. Then, they were ground to powder; dissolved in distilled water and filtrated. The filtrate has been dried in the laboratory oven then kept as the stock material.

Working solutions (1.0 M HCl and 0.5 M H_2SO_4) were prepared from the stock commercial solutions of hydrochloric acid (37%) and sulfuric acid (95%-97%) by dilution with double distilled water.

2.3. Fourier transforms infrared spectroscopy (FT-IR)

The characterization of material by *FT-IR spectroscopy* has been carried out at the Center Pharmaceutical Institute in RABAT using a Perkin Elmer Spectrum apparatus version 10.03.07 ATR with the spectral resolution 4.0 cm^{-1}. The pellet was run from an intimate mixture of sample (1 mg) and potassium bromide (100 mg) under a pressure of 4.5 108 Pa.

2.4. Electrochemical measurements

Electrochemical experiments has been performed using a Potentiostat Radiometer Analytical type PGZ 100 to positive direction using Volta Master 4softwarewhich was controlled by a personal computer coupled with a electrochemical cell containing three-electrode cellin the form of a cylinder of borosilicate glass (Pyrex®) closed by a plug with three electrodes: saturated calomel electrode (SCE), platinum as counter electrode and mild steel samples as working electrode which was cut from a mild steel rod with a cross-sectional area of one cm^2 and embedded in a Teflon holder. Then it was immersed in tests solutions of 1.0 M HCl and 0.5 M H_2SO_4 without and with 100 ppm, 400 ppm, 700 ppm and 1000 ppm of the inhibitor at 25 °C, the open circuit potential was measured after attaining a steady state.

2.4.1. Potentiodynamic polarization measurements

The device used for the potentiodynamic polarization studies Consists of the electrolysis cell. All potentials were measured with respect to SCE. The cell is connected to the potentiometer / Galvanostat, at a scan rate of 1 mV/s after 20 min of immersion time until reaching the steady state. The test solution was thermostat to 25±2 °C in the unburned air atmosphere. In order to determine the polarization curves, different potentials are applied to the working electrode by a counter-electrode, by means of a scanning protocol imposing the increment. The stationary current which is established after the time of study in the electrical circuit between the working electrode and the counter electrode is measured. However, the overall current density, i, is considered as the sum of two contributions, anodic and cathodic

current i_a and i_c, respectively. For the potential domain not too far from the open circuit, we can consider that both processes obey the Tafel law, so we can draw:

$$i = i_a + i_b = i_{corr} \times \{exp[b_a \times (E - E_{corr})] - exp[b_c \times (E - E_{corr})]\} \quad (1)$$

Where i_{corr} is the corrosion current density (A cm^{-2}), and b_a and b_c are respectively the Tafel constant of anodic and cathodic reactions (V^{-1}). These constants are related to the Tafel slope β (V dec^{-1}) in usual logarithmic scale by:

$$\beta = \frac{\ln(10)}{b} = \frac{2.303}{b} \quad (2)$$

The electrochemical parameters, namely the corrosion current density I_{corr}, the extrapolated Tafel slopes anodic βa and cathodic βc, the polarization resistance R_p. The inhibition efficiency (E_{inh} %) are calculated using Eq. 3:

$$\boldsymbol{\eta_{pp}}\,\% = \frac{\boldsymbol{Icorr - Icorr(inh)}}{\boldsymbol{Icorr}} \times 100 \quad (3)$$

Where I_{corr} and $I_{corr(inh)}$ are referred to as the corrosion current density without and with the addition of inhibitor, respectively.

2.4.2. Electrochemical impedance spectroscopy

EIS measurements performed at corrosion potentials, E_{corr}, over a frequency range of 100 kHz to 100 MHz with an AC signal amplitude perturbation of 10 mV peak to peak. The inhibition efficiency (E_{inh} %), are calculated using Eq. 4:

$$\boldsymbol{\eta_{EIS}}\% = \frac{\boldsymbol{Rct(inh) - Rct}}{\boldsymbol{Icorr}} \times 100 \quad (4)$$

Where R_{ct} and R_{ct} (inh) are the charge transfer resistance without and with the addition of the inhibitor, respectively.

All experiments were repeated three times in order to ensure reproducibility. The estimated error did not exceed 10%.

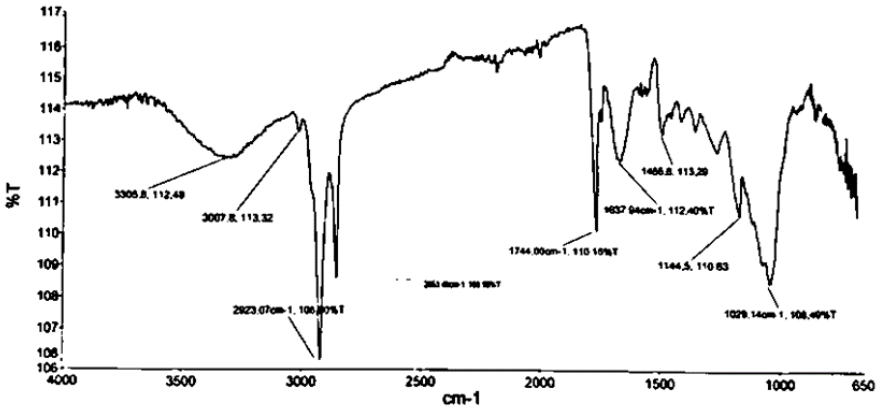

Fig. 2. Infrared spectrum of coriander seeds extracts

Table 2. FT-IR peaks of CSE

Peaks from FT-IR spectra(cm-^{1})	Possible functional groups
3302.5	O-H stretch
2923.05	C-H asymmetric stretch
2853.58	C-H symmetric stretch
1744.81	C=O stretch
1144.5	C-C aliphatic
1028.75	C-O stretch

3. RESULTS AND DISCUSSION

3.1. FTIR results of CSE analysis

The important IR absorption bands of inhibitors are in Fig. 2 and their respective FT-IR peaks are in Table 2. These results showed that the inhibitors containing functional groups with oxygen atoms and other attached to aromatic ring, which are commonly gathered in corrosion inhibitors [13].

3.2. Effects of concentration of CSE on inhibition efficiency and corrosion rate.

3.2.1. Open circuit potential

Fig. 3 presents the open circuit potential (OCP) versus time at different concentration of inhibitor. It is noted that the potential for blank solution stays stable with time. This phenomenon characterizes the corrosion of mild steel with a formation of corrosion products.

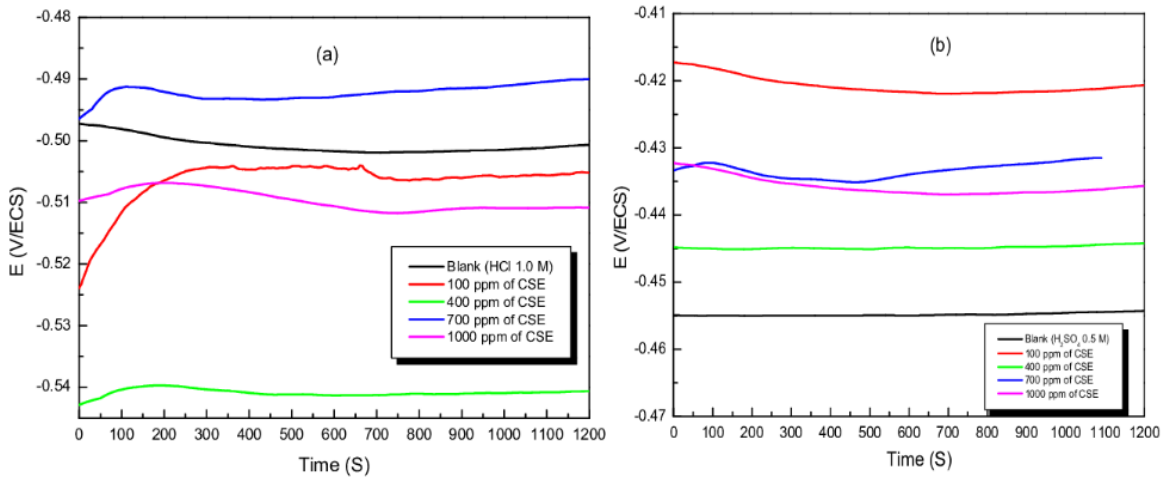

Fig. 3. Evolution of open circuit potential (OCP) versus time for mild steel in **(a)** 1.0 M HCl **(b)** 0.5 M H_2SO_4 with different concentrations of CSE at 298 K

So, in the presence of CSE, the potential shift in the anodic direction and stays quickly stable with time in 0.5 M H_2SO_4 medium, but in the case of 1.0 M HCl, the potential shift in the cathodic direction.

3.2.2. Potentiodynamic polarization

The Tafel polarization curves for mild steel in 1.0 M HCl and 0.5 M H_2SO_4 solution without and with different concentrations (100ppm, 400 ppm, 700 ppm and 1000 ppm) of CSE at 25℃ are shown in Fig. 4.

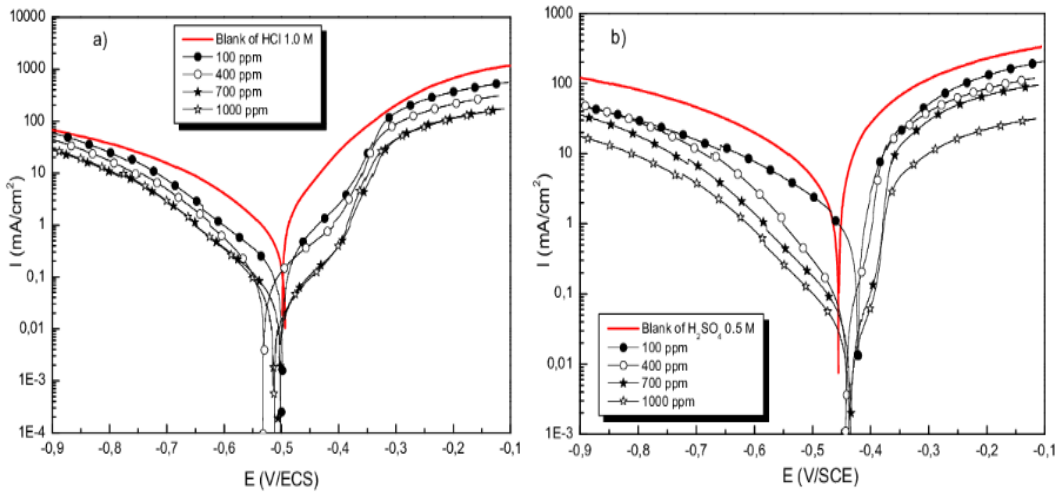

Fig. 4. Tafel polarization curves for mild Steel in **(a)** 1.0 M HCl; **(b)** 0.5 M H_2SO_4 with different concentrations of CSE at 298 K

The electrochemical parameters: anodic Tafel constant (βa), cathodic Tafel constant (βc), corrosion potential (E_{corr}), corrosion current density (I_{corr}), and the corresponding inhibition efficiencies$\eta_{pp}$are illustrated in Table 3.

Table 3. Electrochemical parameters for Mild Steel in 1.0 M HCl and 0.5 M H_2SO_4 with different concentrations of CSE at 298 K

Inhibitor CSE in	Concentration (mg/L)	E_{corr}(mV/ECS)	I_{corr}(μA/cm²)	βc mv	βa mv	η_{pp}%
1.0M HCl	0	-498	983	-92	104	-
	100	-500	170	-80	95	82.7
	400	-540	110	-116	87	88.8
	700	-494	65	-94	80	93.4
	1000	-509	62	-96	77	93.7
0.5M H_2SO_4	0	-451	1850	-99	121	-
	100	-418	652	-108	61	64.7
	400	-438	100	-79	33	94.6
	700	-429	67	-107	37	96.4
	1000	-432	61	-104	40	96.7

Fig. 4 and table 3 showed affected of both anodic and cathodic reactions in the presence of various concentrations of the inhibitor CSE, the cathodic appeared to be more pronounced and the corrosion current densities of the additives decreased significantly compared to the blank. The significant change of Tafel slopes of the anodic (βa) and cathodic (βc) in the presence of CSE can be observed as result of adsorption the molecules of inhibitor. The corrosion process decrease can be explained by both metallic dissolution and hydrogen evolution at the metal surface due to the adsorption of organic compounds (heteroatoms such as oxygen, sulfur, phosphorus and nitrogen) [14-16] found in CSE at the mild steel surface. Those aromatic rings or multiple bonds, found in organic compound acted as mixed type inhibitor, and the inhibition is due to geometric blocking mechanism.

The result obtained in 1.0 M HCl solution containing 1000 ppm of CSE at 25 ℃ indicate the decrease of the corrosion current density of mild steel from 983 μA/cm² to 62 μA/cm² and the increase of corrosion inhibition efficiency to 93.7%, similar results have been obtained in 0.5 H_2SO_4 which we observed that the corrosion current density of mild steel decrease from 1850 μA/cm² to 61 μA/cm² with an efficiency of corrosion inhibition 96.7% and this behaviour can be explained by the good coverage of the metal surface by CSE molecules that block the active sites on the metal surface[17-19].

From all these results, it is clear that the CSE extract have a good inhibitor behaviour for mild steel corrosion in both acidic medium 1.0 M HCl and 0.5 M H_2SO_4.

3.2.3. Impedance spectroscopy (EIS)

The effect of coriander seeds extracts concentration effectuated by Nyquist plots for mild steel in 1.0 M HCl and 0.5 M H_2SO_4 at 298 K was shown in Fig. 5.

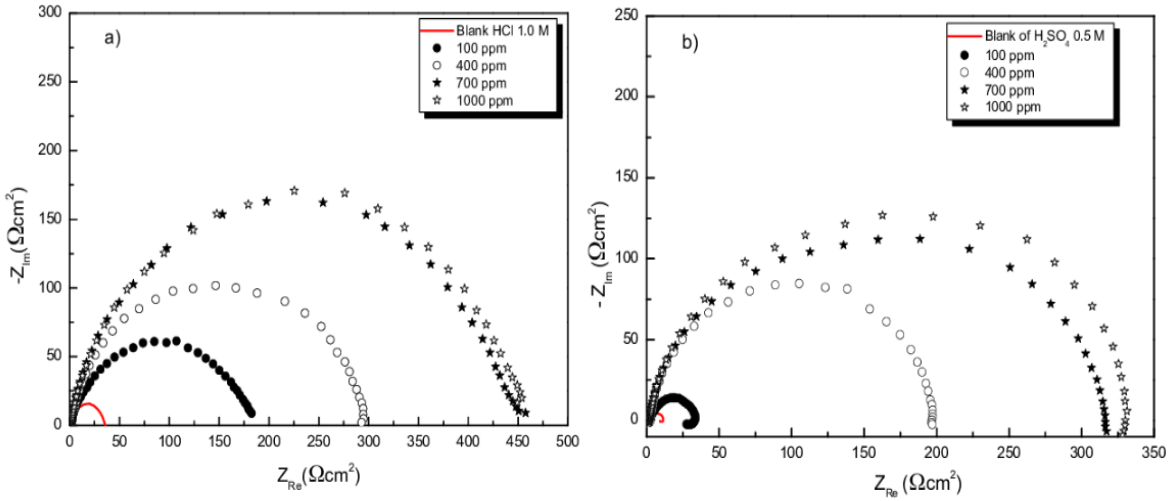

Fig. 5. Impedance diagrams for Mild Steel in **(a)** 1.0 M HCl and **(b)** 0.5 M H_2SO_4 with different concentrations of CSE at 25 ºC

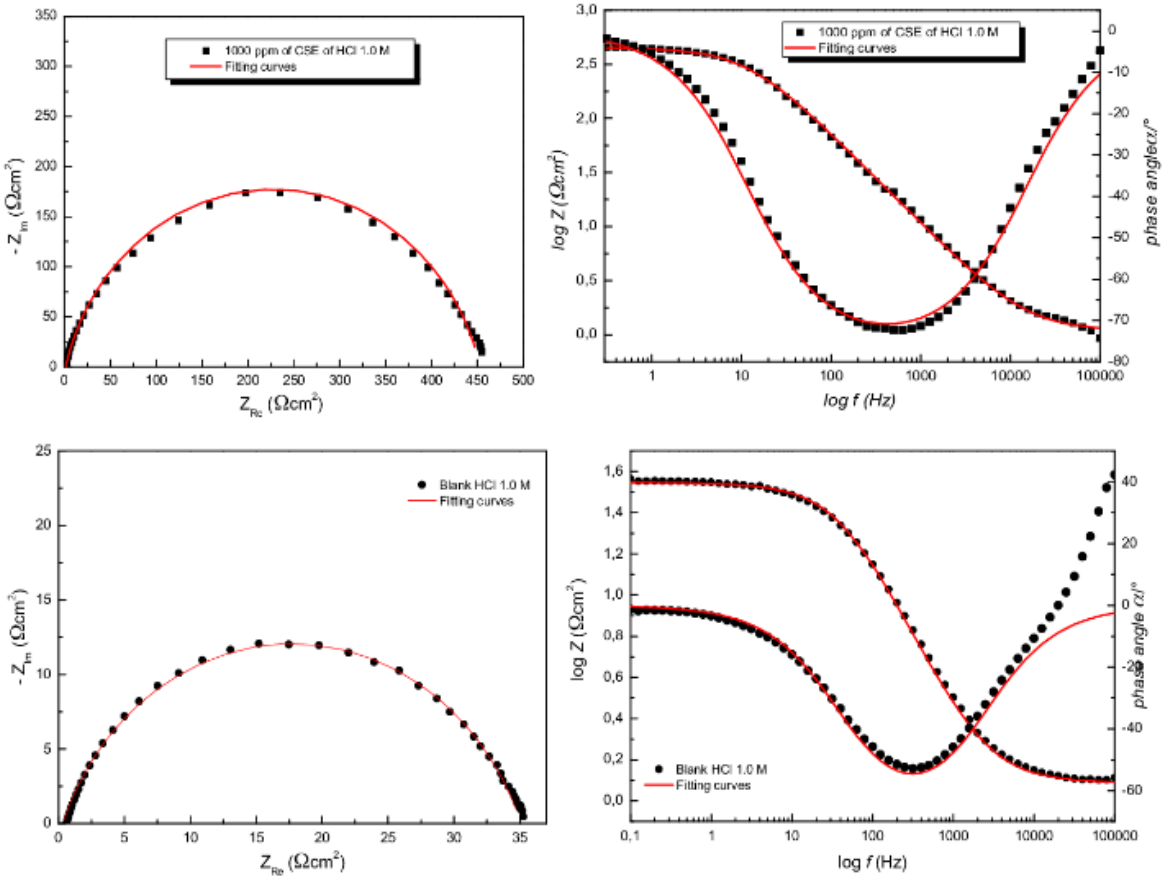

Fig. 6. Nyquist and Bode plot for mild steel in 1M HCl with and without 1000 ppm of CSE at 298 K

The Nyquist and Bode plots of both experimental and simulated data of mild steel in 1.0 M HCl solution without and with 1000 ppm of CSE are shown in Fig. 6.

The Nyquist and Bode plots of both experimental and simulated data of mild steel in 0.5 M H_2SO_4 solution without and with 1000 ppm of CSE are shown in Fig. 7.

Based on the findings of Nyquist and bode plots, two electrical equivalent circuits, which is given in Fig.8 was used to model the mild steel/solution interface. It is clear that the impedance plots are in accordance with those calculated by the used equivalent circuit model. Most of the impedance curves obtained for the corrosion of mild steel in 1.0 M HCl and 0.5 M H_2SO_4 solutions with the inhibitor consist of two capacitive loops, with their centres at the real axis and their diameters increase with the increase of the inhibitor concentration, which indicates that the surface covered by CSE increases with the increase of CSE concentration. The presence of two capacitive loops may be attributed to the relaxation process obtained by adsorption species like Cl^-_{ads}, $SO_4^{2-}{}_{ads}$and H^+_{ads} on the electrode surface [20,21].

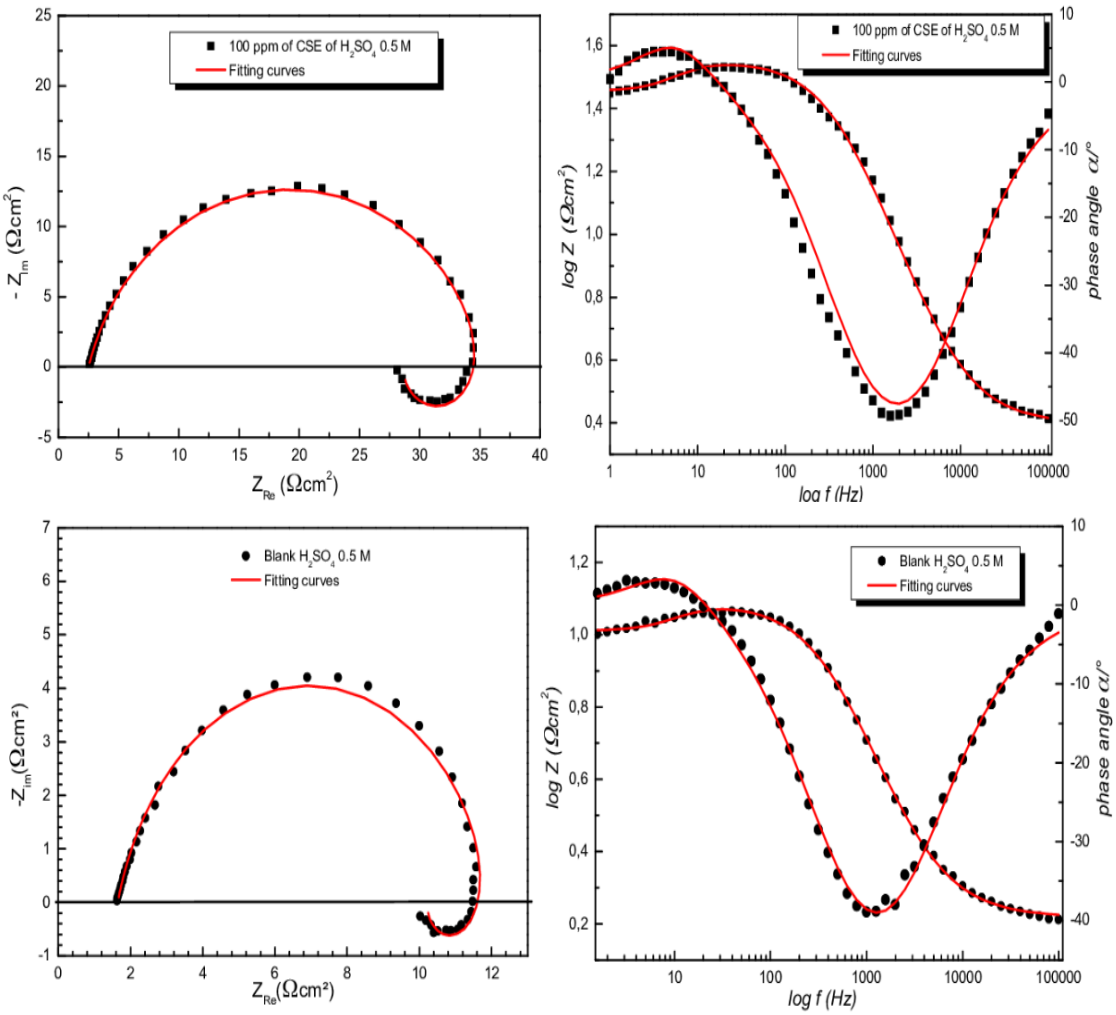

Fig. 7. Nyquist and Bode plot for mild steel in 0.5 M H_2SO_4 with and without 100 ppm of CSE at 298 K

In other words, the inductive behaviour at low frequency is probably due to the adsorption of the products of the corrosion on the electrode, all parameters were obtained from the high capacitive loops. This is manifested in the increase in R_{ct} values and with a simultaneous decrease in the values of C_{dl} (Table 4). The increase in double layer thickness resulted in the decrease in C_{dl} that will lead to decrease in dielectric constant as a result of displacing the adsorbed water molecules and adsorption of extract (organic matter) on to the surface of the mild steel [22,23].

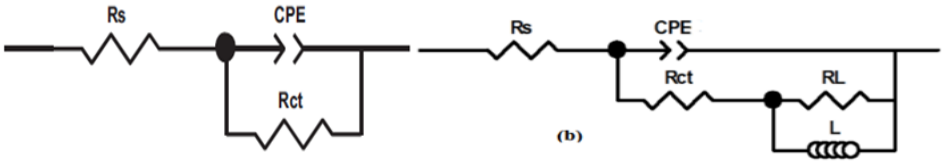

Fig. 8. Electrical equivalent circuits used for modeling the interface of mild steel /(a) 1M HCl and / (b) 0.5 M H_2SO_4

Table 4. Impedance parameters for Mild Steel in 1.0 M HCl and 0.5 M H_2SO_4 with different concentrations of CSE at 25 ºC

Medium	**Concentration (ppm)**	**R_{ct} (Ω.cm²)**	**C_{dl}(µF/cm²)**	**η_{EIS}%**
1.0 M HCl	0	35	298	-
	100	185	140	81.1
	400	298	100	88.2
	700	452	55	92.2
	1000	457	50	92.3
0.5M H_2SO_4	0	11.7	10480	-
	100	32.6	123	64
	400	199	118	94
	700	312	91	96.2
	1000	328	75	96.4

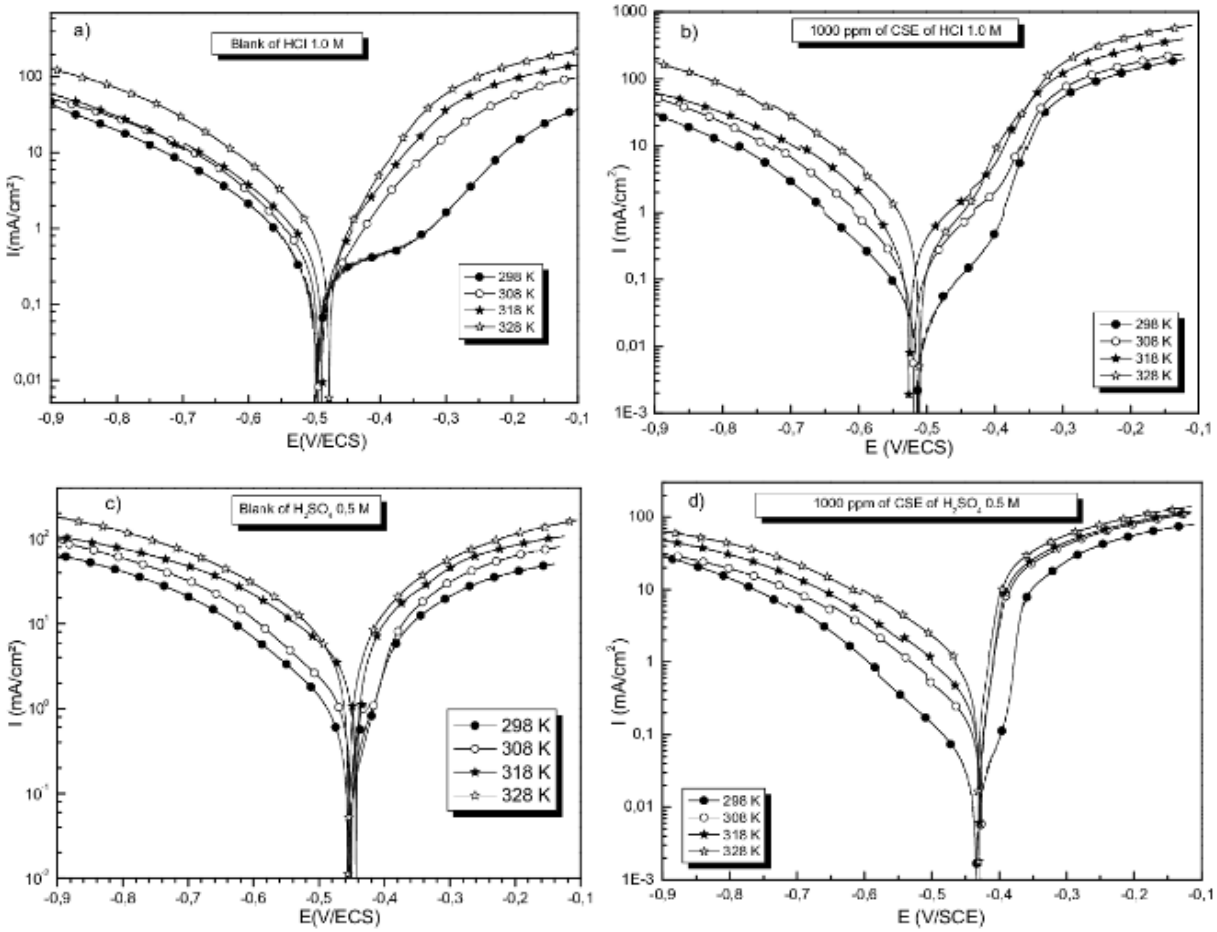

Fig. 9. Tafel polarization curves for mild Steel in 1.0 M HCl in absence**(a)** and presence of CSE**(b)** and 0.5 M H_2SO_4 in absence**(c)** and presence of CSE**(d)** with different temperatures

Following both the polarization and EIS studies, it was observed that inhibition efficiency increased with the increase in the concentration of CSE (Tables 3 and 4) reaching the maximum values of 85.62% and 83.05% at 60% CSE extract in 1.0 M HCl and 0.5 M H_2SO_4, respectively, due to the increase of the adsorption of inhibitor molecules at the active sites on the mild steel surface under such condition. The efficiency of CSE was good compared to the previous studies investigated by other materials.

3.3. Effect of temperature on inhibition efficiency and corrosion rate

Fig. 9 represents the polarization curves of mild steel in the presence of 1000 ppm of coriander seeds extracts at different temperatures (298, 308, 318 and 328K) in the acidic medium 1.0 M HCl and 0.5 M H_2SO_4

Table 5. Electrochemical parameters for Mild Steel in 1.0 M HCl and 0.5 M H_2SO_4 with different temperatures

		T(k)	E_{corr} (mV/ECS)	I_{corr} (μA/cm²)	β_c (mv)	β_a (mv)	η_{EIS}%
1.0 M HCl	**Blank**	298	-498	983	-92	104	-
		308	-491	1200	-184	112	-
		318	-475	1450	-171	124	-
		328	-465	2200	-161	118	-
	Inhibitor	298	-509	62	-96	77	93.7
		308	-514	92	-88	82	92.3
		318	-523	160	-69	96	89
		328	-510	280	-60	100	87.3
0.5 M H_2SO_4	**Blank**	298	-451	1850	-87	124	-
		308	-453	2250	-92	114	-
		318	-449	2480	-96	102	-
		328	-442	3340	-102	97	-
	Inhibitor	298	-432	61	-104	40	96.7
		308	-423	120	-99	150	94.6
		318	-425	168	-86	134	93.2
		328	-427	282	-132	97	91.5

The values of the corrosion potential (E_{corr}), the corrosion current density (I_{corr}), the βc and anodic βa cathode slopes and the inhibition efficiency (η_{EIS}) are shown in Table 5. The inhibition efficiency decreased with the increase of temperature from 93.7% to 87.3% in the 1.0 M hydrochloric medium and from 96.7% to 91.5% for the 0.5 M sulfuric medium.

3.4. Thermodynamic study

The thermodynamic study makes it possible to quantify the inhibition efficiency against corrosion and facilitates the calculation of the thermodynamic parameters and the activation energy in order to determine and interpret the type of adsorption adopted by the inhibitor.

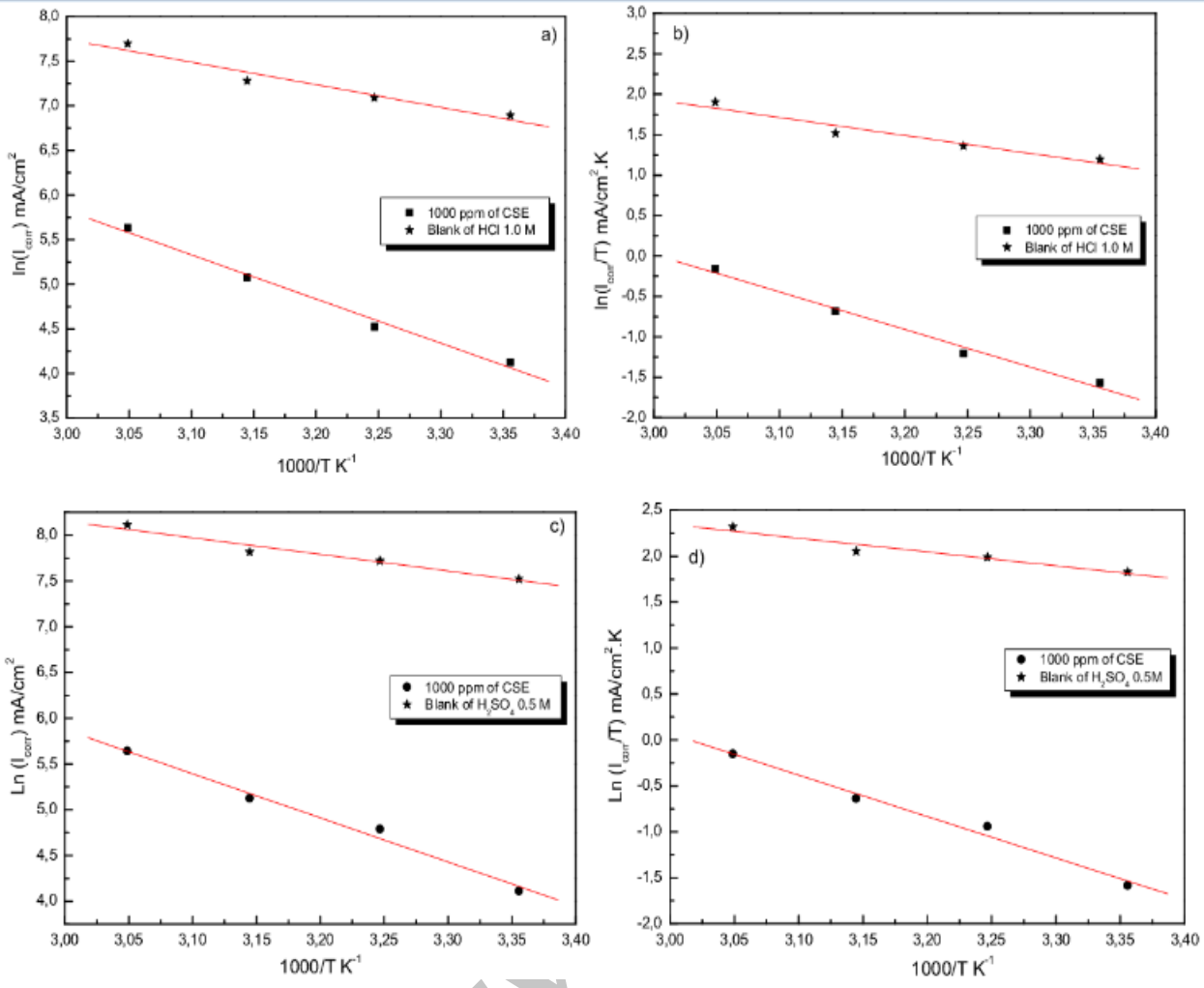

Fig. 10. Arrhenius curves corresponding to the corrosion of mild steel in 1.0 M HCl (a, b) and 0.5 M H_2SO_4(c, d) in absence and presence of CSE

The Arrhenius curves are plotted by calculating the logarithm of the corrosion rates (LnI_{corr}) with respect to the absolute temperature (1/T) for the acidic medium 1.0 M HCl and 0.5 M H_2SO_4 (Fig. 10) Arrhenius equation (5)[24]:

$$\boldsymbol{ln\ Icorr = -\frac{Ea}{RT} + ln\ A} \qquad (5)$$

Where A is the pre-exponential constant of Arrhenius, R is the universal gas constant, E_a is the apparent activation energy, and T is the absolute temperature.

From the (Table 6), E_a increases with the addition of CSE over the control solutions. The change in corrosion rate with temperature increase was studied in 1.0 M HCl and 0.5 M H_2SO_4 media in the absence and presence of 1000ppm of the inhibitor. Table 6 contains the different data obtained from the curves and equation (3).

The increase in corrosion rate is more shown with the increase for both acid solutions in the absence of CSE. After the addition of CSE, the corrosion rate decreases rapidly.

The standard enthalpy of adsorption (ΔH_a) can be calculated using the equation of Van't Hoff's isobar (6):

$$\frac{dln\, K_a}{dT} = \frac{\Delta H_a}{RT^2} \quad (6)$$

The entropy values (ΔS_a) are derived from the Gibbs-Helmholtz relation (7):

$$\mathbf{\Delta G_a = \Delta H_a - T\Delta S_a} \quad (7)$$

The free energy of adsorption (ΔG_a) can be given by equation (8):

$$\boldsymbol{\Delta G_a = - RT\, ln\, K_a\, Cs} \quad (8)$$

R:the universal gas constant=8.314 J K^{-1} mol^{-1}.
T: the ambient temperature is 298 ° K.
Cs: the concentration of water=1 M.

The values of the adsorption energies (ΔG_a, ΔH_a and ΔS_a) are grouped in the table 6. From the results, it is noted that the value of the enthalpyΔH_a calculated from equation (4) is 38.5 kJ/mol in the 1.0 M HCl medium and 37.5 kJ/mol in 0.5 M H_2SO_4 medium, which shows the endothermic nature of the adsorption on the surface of the mild steel. This confirms the previous result (the molecules of this extract are the molecules of this extract are physically adsorbed on the surface of this metal), it can also be explained by the decrease in the inhibition efficiency by increasing the temperature and consequently an increase in the standard energy of adsorption.

Table 6. Activation parameters for mildsteel in HCl1.0 M and H_2SO_4 0.5 M

Medium	Concentrations	E_a KJ/mol	ΔH_a KJ/mol	ΔS_aKJ/mol
HCl 1.0 M	Blank	21	18.5	-126
	1000 ppm	41	38.5	-82
H_2SO_4 0.5 M	Blank	15	12.5	-140.5
	1000 ppm	40.12	37.5	-84.4

The entropy value increased from -126 to -82 kJ/mol in 1.0 M HCl medium and from -140.5 to -84.4 kJ/mol in 0.5 M H_2SO_4 medium, with 1000 ppm of the inhibitor. This can be attributed by the increase in the degree of disorder before the adsorption of the extract on the steel [25,26]. On the other hand, when the molecules are adsorbed on the surface of the substrate, there will be a decrease in the disorder after a decrease in the entropy [27,28].

3.5. Adsorption Isotherms

The mode and extent of the interaction between the inhibitor and the mild steel surfaces were investigated by applying adsorption isotherms. The Langmuir, Freundlich, and Temkin approach were used to determine the adsorption mechanisms of the inhibition reaction.

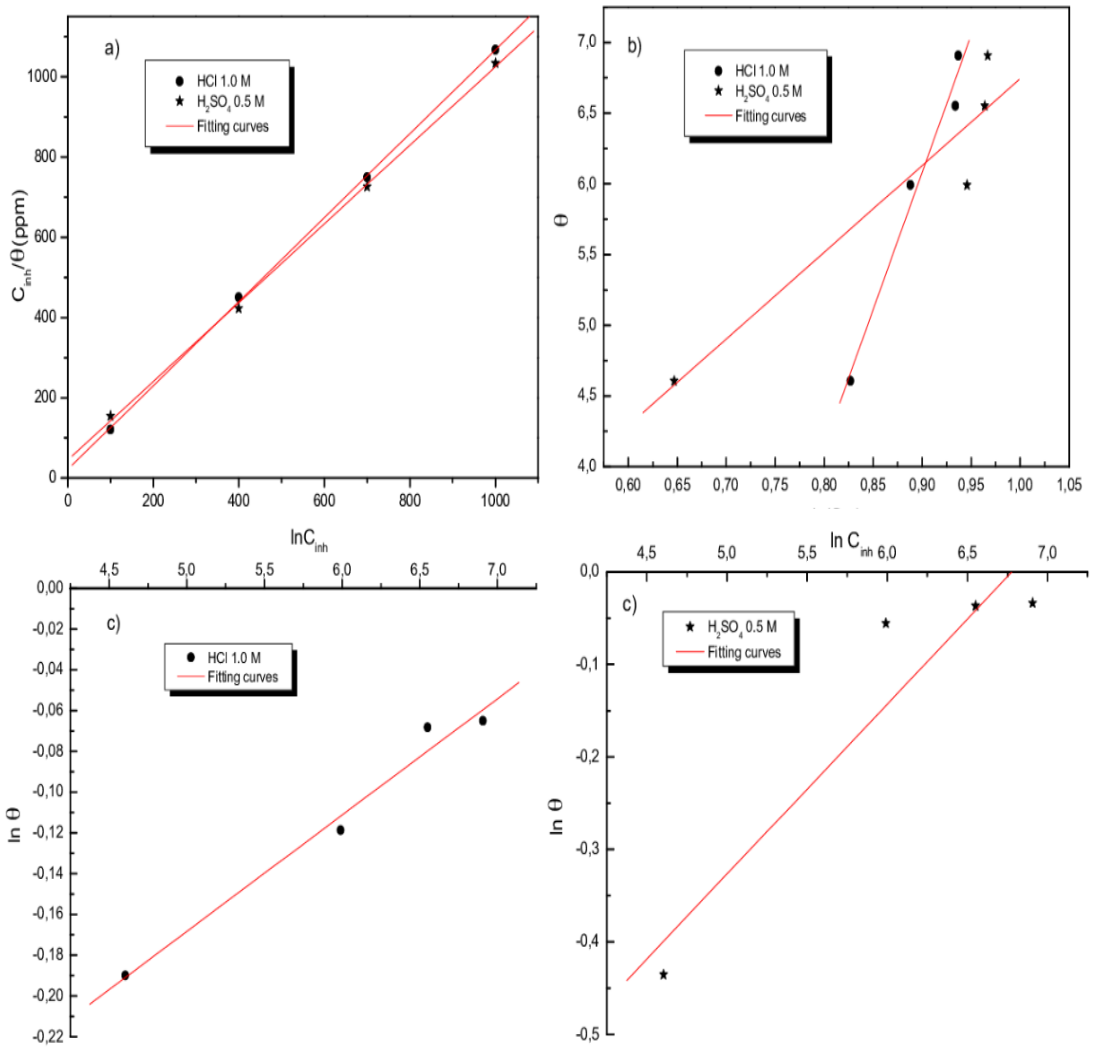

Fig. 11. Langmuir (a); Temkin (b) and Freundlich (c) isotherms for the adsorption of CSE extract on the surface of the mild steel respectively in 1.0 M HCl and0.5 M H_2SO_4

The isotherms were best described by the adsorption behavior of the CSE extracts on the surface of mild steel. Langmuir adsorption isotherm can be expressed according to Eq. 9 [29]:

$$\boldsymbol{\theta} = \frac{\mathbf{Kads\ Cinh}}{\mathbf{1+Kads\ Cinh}} \quad (9)$$

Where C_{inh} is the inhibitor concentration, K_{ads} is the adsorption equilibrium constant. Rearranging this Eq. 7 gives Eq. 10:

$$\frac{\mathbf{Cinh}}{\theta} = \frac{1}{\mathbf{Kads}} + \boldsymbol{K_{ads}} \quad (10)$$

The linear variation of C_{inh}/θ *vs.* C_{inh} of the CSE in 1.0 M HCl and in 0.5 M H_2SO_4 solutions showed that the adsorption is well fitted by the Langmuir.
The equation 11 of the Freundlich isotherm is:

$$\boldsymbol{ln\theta = lnK_{ads} + \frac{1}{n} lnC_{inh}} \quad (11)$$

K_{ads} and n are constants for given adsorbate and adsorbing at a particular temperature.

According the Temkin model, the free adsorption energy of the adsorbate is a linear function of the overlapping rate θ and the chemical rate constants are a function of θ. There is attraction or repulsion between species adsorbed on the surface. The equation 12 of the Temkin isotherm is:

$$\boldsymbol{\theta = \frac{1}{f} lnKads + \frac{1}{f} lnC_{inh}} \quad (12)$$

f denotes the adsorbent-adsorbate interaction.
C_{inh} is the inhibitor concentration in the electrolyte.

The degree of surface coverage (θ) can readily be calculated from Equations (8) to (9). That degree is numerically identical to the value of percentage inhibition efficiency. Where *C* is the concentration of the inhibitor and K_{ads} represents the adsorption equilibrium constant. The plots of C/θversus *C* yield a straight line proving that experimental results are in good agreement with the three adsorption isotherms (Fig.11). From table 7, the increasing value of K_{ads} in the case of 1.0 M HCl medium reflects the increasing adsorption capability, due to structural formation, on the metal surface [30].

The study of the adsorption isotherms Langmuir, Freundlich and Temkin of CSE in the acidic medium 1.0 M HCl and 0.5 M H_2SO_4 shows that the adsorption obey all of the studied isotherms [31].

Table 7. Isotherms parameters of adsorption of CSE by mild steel

Adsorption isotherms	**Medium**	**R^2**	**Slope**	**K_{ads}**
Langmuir	1.0 M HCl	0.99984	1.098	0.048
	H_2SO_4 0.5M	0.99949	0.894	0.018
Freundlich	HCl 1.0 M	0.98944	0.051	0.635
	H_2SO_4 0.5M	0.94456	0.274	0.288
Temkin	HCl 1.0 M	0.98824	0.044	0.182
	H_2SO_4 0.5M	0.94769	0.216	24573.17

On the basis of characterization of CSE, we postulate that the major constituents act together by adsorption to ensure inhibition. Then, the inhibition is regarded as intermolecular synergistic effect of various compounds of the extract. It is adequately recommended to not determine ΔG_{ads} values since the mechanism of adsorption remains unknown [32].

3.6. Scanning electron microscopy (SEM)

SEM microphotographs of the surface of the mild steel coupons after in 1.0 M HCl solution and in 0.5 M H_2SO_4 in the absence and presence of CSE are revealed in Figs 12 and 13. The microphotographs of mild steel surface in the absence of inhibitor are given in Fig. 12.a and fig.13.a represent the polished metal sample; the whole surface is a plane. Fig. 12.b and fig .13.b represent the inhibited samples immersed for 12 h in 1.0 M HCl and 0.5 M H_2SO_4 containing optimum concentration of the inhibitor. These figures confirm the formation of a protective film by CSE on the mild steel surface in both acid solutions [33].

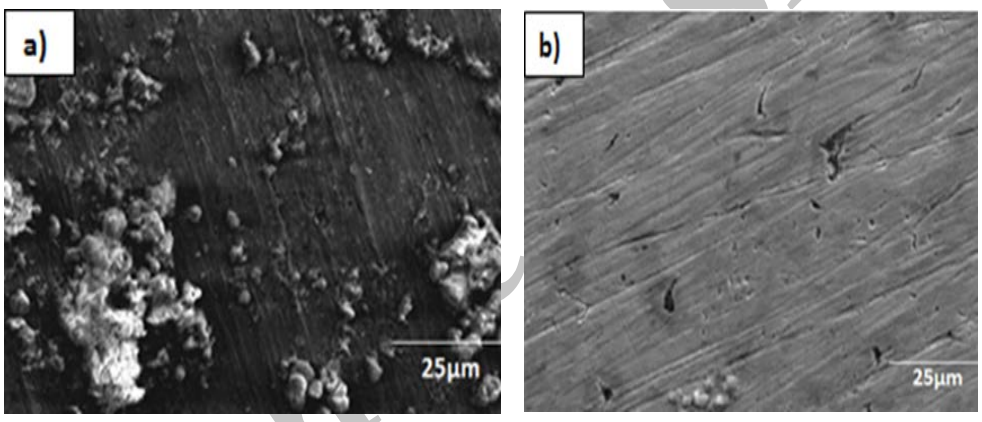

Fig. 12. SEM microphotographs of mild steel in 1.0 M HCl without (a) and with (b) CSE after 12 h of immersion

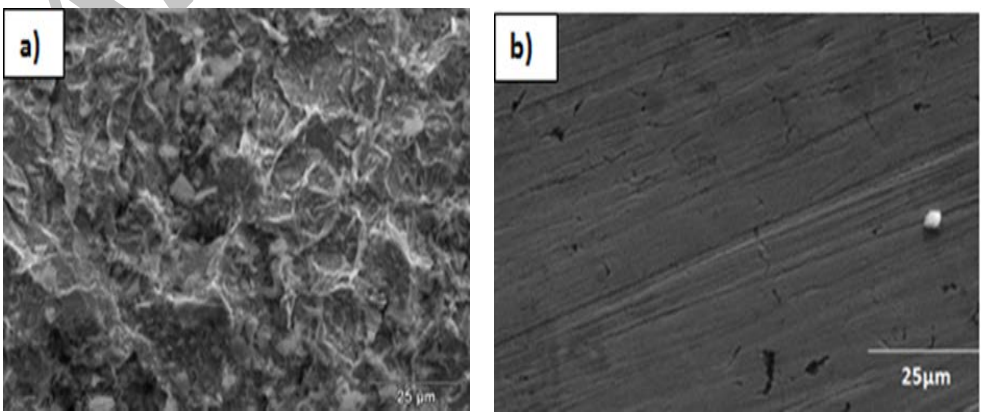

Fig. 13. SEM microphotographs of mild steel in 0.5 M H_2SO_4 without (a) and with (b) CSE after 12 h of immersion

4. CONCLUSION

To sum up, the spectroscopic, electrochemical and thermodynamic results corresponding to mechanisms of coriander seeds extracts CSE as a corrosion inhibitor for mild steel in acidic medium 1.0 M HCl and 0.5 M H2SO4 can be explained as that the inhibitor contains the functional groups containing oxygen O and other aromatic components, which explains the effect Inhibitor of these extracts. The extracts of CSE act on the cathode and anode kinetics. They are therefore mixed inhibitors. Also, the inhibition efficiency increases with the increase of concentration with a maximum efficiency at a concentration of 1000 ppm at 25°C for both mediums. Furthermore, the study as a function of the temperature showed that the inhibitory efficiency decreases with the increase of the temperature and that the adsorption of the extracts is done by physical adsorption. The thermodynamic data calculated for the extracts of coriander grains confirm the physical adsorption of these extracts on the metal surface for the two acid media 1.0 M HCl and 0.5 M H2SO4. Moreover, the study of the adsorption isotherms Langmuir, Freundlich and Temkin of CSE in the acidic medium1.0 M HCl and 0.5 M H2SO4 shows that the adsorption obey all of the studied isotherms. Finally, SEM method confirmed all previous results and showed that the corrosion of mild steel in 1.0 M HCl and 0.5 M H2SO4 could be inhibited by CSE.

REFERENCES

[1] M. N. I. Bhuiyan, J. Begum, and M. Sultana, Bangladesh J. Pharmacol. 4 (2009) 2.
[2] M. Salasi, T. Shahrabi, E. Roayaei, and M. Aliofkhazraei, Mater. Chem. Phys. 104 (2007).
[3] P. Bommersbach, C. Alemany-Dumont, J. P. Millet, and B. Normand, Electrochim. Acta 51 (2005).
[4] M. Traisnel, Université des Antilles et de la Guyane, Thesis (2013).
[5] L. Wang, Corros. Sci. 48 (2006) 3.
[6] E. I. Ating, S. A. Umoren, I. I. Udousoro, E. E. Ebenso, and A. P. Udoh, Green Chem. Lett. Rev. 3 (2010) 2.
[7] A. Nahlé, JMES 7 (2016) 3118.
[8] O. K. Abiola, and A. O. James, Corros. Sci. 52 (2010) 2.
[9] P. C. Okafor, M. E. Ikpi, I. E. Uwah, E. E. Ebenso, U. J. Ekpe, and S. A. Umoren, Corros. Sci. 50 (2008) 8.
[10] O. Benali, H. Benmehdi, O. Hasnaoui, C. Selles, and R. Salghi, J. Mater. Env. Sci. 4 (2013) 1.
[11] O. K. Abiola, J. O. E. Otaigbe, and O. J. Kio, Corros. Sci. 51 (2009) 8.
[12] K. Dahmani, M. Galai, M. Cherkaoui, A. El hasnaoui, and A. El Hessni, J. Mater. Environ. Sci. 8 (2017) 1676.
[13] G. M. AL-Senani, S. I. AL-Saeedi, and R. S. AL-Mufarij, J. Mater. Env. Sci. 7 (2016).

[14] K. Alaoui, Y. El Kacimi, M. Galai, K. Dahmani, R. Touir, A. El Harfi, M. EbnTouhami, Anal. Bioanal.Electrochem. 8 (2016) 830.
[15] M. Lashgari, M. R. Arshadi, G. A. Parsafar, and V. S. Sastri, Corrosion 62 (2006) 3.
[16] C. Gabrielli, M. Keddam, and H. Takenouti, Matériaux and Techniques 95 (2007) 385.
[17] M. Galai, M. El Gouri, O. Dagdag, Y. El Kacimi, A. Elharfi, and M. Ebn Touhami, J. Mater. Environ. Sci. 7 (2016) 1562.
[18] M. Moradi, J. Duan, and X. Du, Corros. Sci. 69 (2013) 338.
[19] Y. Tang, F. Zhang, S. Huc, Z. Cao, Z. Wu, and W. Jing, Corros. Sci.74 (2013) 271.
[20] A. K. Singh, and M. A. Quraishi, Corros. Sci. 52 (2010) 152.
[21] P. Li, T. C. Tan, T. Y. Lee, Corros. Sci. 38 (1996) 1935.
[22] M. Galai, M. Rbaa, Y. El Kacimi, M. Ouakki, N. Dkhirech, R. Touir, B. Lakhrissi, M. Ebn Touhami, Anal. Bioanal. Electrochem. 9 (2017) 80.
[23] M. Galai, M. El Faydy, Y. El Kacimi, K. Dahmani, K. Alaoui, R. Touir, B. Lakhrissi, and M. Ebn Touhami, Portugaliae Electrochim. Acta. 35 (2017) 233.
[24] R. Raicheff, K. Valcheva, and E. Lazarova, Proceeding of the Seventh European Symposium on Corrosion Inhibitors, Ferrara, Italy (1990) 48.
[25] L. Herrag, B. Hammouti, S. Elkadiri, A. Aouniti, C. Jama, H. Vezin, and F. Bentiss, Corros. Sci. 52 (2010) 3042.
[26] S. Martinez, and I. Stern, Appl Surf Sci. 199 (2002) 83.
[27] J. Marsh, Advanced Organic Chemistry. 3rd ed. New Delhi: Wiley Eastern, (1988).
[28] K. Dahmani, M. Galai, A. Elhasnaoui, B. Temmar, A. El Hessni, and M. Cherkaoui, Der Pharm. Chem. 7 (2015) 566.
[29] I. Langmuir, Am J. Chem. Soc. 40 (1918) 1361.
[30] A. A. El-Awady, B. A. Abd-El-Nabey, and S. G. Aziz, J. Electrochem. Soc. 139 (1992) 2149.
[31] A. Ouass, I. Ismi, H. Elaidi, E.H. Rifi, and A. Lebkiri, J. Mater. Environ. Sci. 8 (2017) 3448.
[32] S. Rekkab , H. Zarrok , R. Salghi, A. Zarrouk, Lh. Bazzi , B. Hammouti, Z. Kabouche, R. Touzani, and M. Zougagh, J. Mater. Environ. Sci. 3 (2012) 4.
[33] R. A. Prabhu, T. V. Venkatesha, A. V. Shanbhag, G. M. Kulkarni, and R. G. kalkhambkar, Corros. Sci. 50 (2008) 3356.